ELSEVIER

Materials Science and Engineering A 417 (2006) 315–321

MATERIALS SCIENCE & ENGINEERING A

www.elsevier.com/locate/msea

The microstructure, tensile properties, and creep behavior of Mg–Zn alloys containing 0–4.4 wt.% Zn

C.J. Boehlert [a,*], K. Knittel [b]

[a] *Michigan State University, Department of Chemical Engineering and Materials Science, 2527 Engineering Building, East Lansing, MI 48824-1226, USA*

[b] *Advanced Ceramics Research, Incorporated, Tucson, AZ 85706, USA*

Accepted 2 November 2005

Abstract

This paper describes the microstructure, tensile, and tensile–creep behavior of a series of Mg–Zn alloys ranging from 0 to 4.4 wt.% Zn. The microstructures consisted of equiaxed hexagonal-close-packed grains with fine precipitates preferentially located at grain boundaries. Some of the microstructures contained fine laths within the equiaxed grains. The finest grain sizes were observed for a Zn composition of 4 wt.%. Tensile experiments were performed at room temperature and 150 °C while creep experiments were conducted at 150 °C for applied stresses between 30 and 50 MPa. The greatest tensile and creep resistance was exhibited by Mg–4.1Zn which contained 0.2 wt.% Y. The measured creep exponent for the Mg–4.1Zn alloy was 4.2, suggesting dislocation climb as the dominant creep mechanism. Overall, Zn proved to be a potent grain refiner and strengthener for Mg where 4 wt.% appeared to be the optimal Zn content for tensile and creep strengthening over the range of alloying additions examined.

Keywords: Lightweight alloys; Tension; Creep; Microstructure; Magnesium

1. Introduction

Magnesium (Mg) alloys display a promising balance of properties including low density, good specific strength and stiffness, good processability, and adequate ductility. Because of these attractive properties, Mg alloys have been considered for lightweight automotive structural components for improving fuel efficiency. However, their poor creep resistance and limited temperature capability have restricted their widespread application. In order to improve their creep strength, rare earth and/or alkaline earth elements in small quantities have been effectively used as alloy additions [1–14]. In addition, Zn in low quantities has also proven to aid tensile and creep strength, especially when combined with yttrium (Y) [13–18]. A small concentration of Zn (as low as 0.05 wt.%) can provide a significant strengthening effect in Mg–Y alloys [13,17]. However, rare earths and alkaline earth elements are expensive and dense alloying additions and in the case of Y, metastable rare earth precipitates are unstable at elevated temperature and grow fast or transform to equilibrium precipitates which have negative effects on strengthening [19]. A high Y content is required to obtain a high density of metastable precipitates. Thus from a weight savings point of view it would be beneficial to develop Mg alloys with lower Y contents for structural applications, where creep strength is important. This work concentrated primarily on the effect of Zn concentration, between 0 and 4.4 wt.%, on the room temperature (RT) and 150 °C tensile and tensile–creep behavior. In addition, a small concentration of Y was added to a Mg–4.1Zn alloy and its tensile and creep behavior was characterized.

2. Experimental procedures

2.1. Materials and processing

The different alloy compositions evaluated were Mg–2.9Zn, Mg–3.3Zn, Mg–4.0Zn, Mg–4.1Zn-0.2Y, and Mg–4.4Zn.[1]

* Corresponding author. Tel.: +1 517 353 3703; fax: +1 517 432 1105.
E-mail address: boehlert@egr.msu.edu (C.J. Boehlert).

[1] All alloy compositions are given in weight percent.

0921-5093/$ – see front matter © 2005 Elsevier B.V. All rights reserved.
doi:10.1016/j.msea.2005.11.006

Table 1
Measured compositions and grain sizes of the alloys studied

Alloy	Wt.% Zn	Wt.% Y	Wt.% Zr	Grain size (μm)
Mg	0.017		0.003	242.6
Mg–2.9Zn	2.93		<0.001	106.5
Mg–3.3Zn	3.30		<0.001	155.6
Mg–4.0Zn	3.98		0.052	70.2
Mg–4.1Zn–0.2Y	4.10	0.20	0.002	77.8
Mg–4.4Zn	4.44	<0.001		112.9

Chemical composition (Table 1) was determined by using inductively coupled plasma and mass spectroscopy techniques. Each alloy was prepared at Advanced Ceramics Research, Incorporated (Tucson, AZ, USA). After the Mg and Zn powders were blended, the compositions were hot pressed at 28 MPa for 1–2 h at 535 °C into a block using a 75 mm × 75 mm × 25 mm die. In addition to the alloys fabricated, a coupon of Mg (98% purity) was fabricated using the same processing conditions. It was noted that this processing technique did not result in fully-homogeneous microstructure as some chemical segregation remained. However, no post processing was performed and very little porosity was observed. Each of the blocks was either electrodischarge machined or milled into a dogbone design for mechanical testing based on ASTM C 1161. Fig. 1a and b illustrates an as-processed block and the associated tensile dogbone samples.

2.2. Metallographic sample preparation and microstructural characterization

Metallographic samples were cut using a low-speed diamond saw then mounted in a polymeric resin for polishing preparation. The mounts were polished using diamond paste, diamond thinner, and ethanol. Final polishing included 1 μm diamond paste for 30 min. Microstructural analysis was performed using a Quanta 200 Field Emission Gun Environmental Scanning Electron Microscope (ESEM) equipped with an EDS detector for elemental analysis. Grain size (d) was determined using the mean line-intercept method according to ASTM standard E112 [20], where over 50 grains were measured per sample and the average grain size was calculated. Fracture surfaces were examined in SEM using failed samples from both the tensile and tensile–creep testing.

2.3. Mechanical testing

Both RT and 150 °C tension experiments were performed in air at a strain rate of $10^{-3}\,s^{-1}$ using an Instron 8562 mechanical testing machine. The ultimate tensile stress (UTS), 0.2% offset yield stress (YS), and elongation at failure (ε_f) were recorded for each test. Up to five specimens per alloy were tensile tested and the reported properties were averaged. Open-air tensile–creep experiments were performed on either of the two vertical Applied Test System, Incorporated load frames containing a 20:1 lever–arm ratio. The testing temperature was 150 °C, and the stresses ranged between 30 and 50 MPa. The experiments were performed under constant load. In most cases, the reduction in cross-sectional area was not sufficient to significantly alter the stress; therefore, the stresses were assumed to be constant. Specimen temperatures were monitored by three chromel–alumel type K thermocouples located within the specimen's reduced section to maintain a temperature control of ±2 °C. The experiments were conducted such that the specimens were soaked at the creep temperature for at least 30 min prior to applying load in order to minimize the thermal stresses. Tensile displacement was measured using an extensometer/linear variable differential transducer coupling, and the temperature–strain–time data were collected. After the creep strain had proceeded well into the secondary regime, either the load or temperature was changed or the creep test was discontinued. The tested specimens were cooled under load to minimize the recovery of the deformed structures. Selected specimens were taken to failure.

3. Results and discussion

3.1. Microstructure

Fig. 2a–f is a set of backscatter electron SEM micrographs illustrating the as-processed alloy microstructures. The alloys exhibited equiaxed grains with precipitates, of greater density than the matrix, decorating the grain boundaries. Fig. 3a illustrates that for an Mg–4.1Zn–0.2Y alloy, the lighter particles at the grain boundaries contained Zr. It is noted that 0.002 wt.% Zr was present in this alloy (see Table 1) as a small quantity of Zr powders were present in the initial blended materials. The matrix was enriched in Mg and Zn, see Fig. 3b, however, fine nanometer size laths/platelets were exhibited within the equiaxed grains for the Mg–2.9Zn and Mg–4.1Zn–0.2Y alloys, Fig. 4a and b, where

(a) (b)

Fig. 1. Illustration of an (a) as-processed block and (b) machined tensile dogbones.

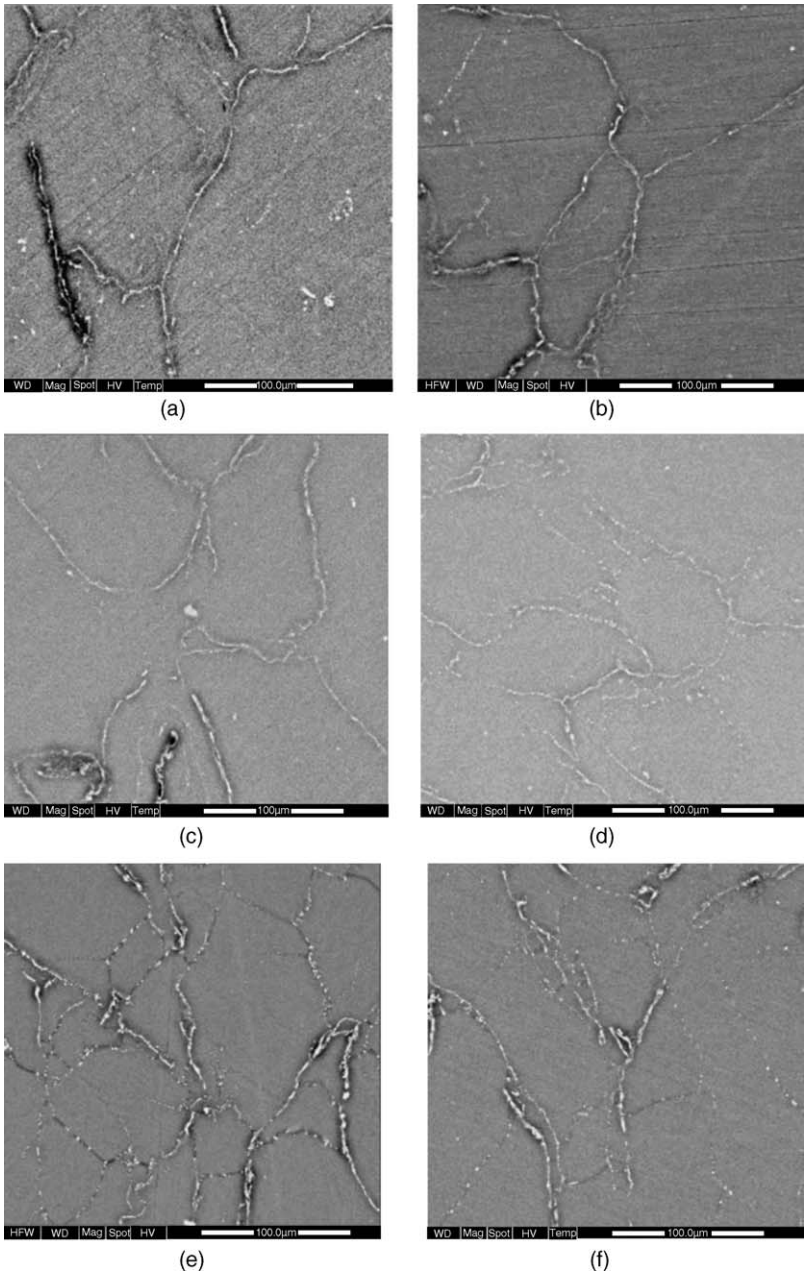

Fig. 2. BSE SEM images of the studied materials: (a) 0Zn, (b) 2.9Zn, (c) 3.3Zn, (d) 4.0Zn, (e) 4.1Zn–0.2Y, and (f) 4.4Zn.

the laths were finer than the resolution of the EDS technique. The equiaxed grain sizes of the Mg–Zn alloys, listed in Table 1, ranged between 70 and 155 μm and varied as a function of alloy composition. The Mg–4.1Zn–0.2Y and Mg–4.0Zn alloys exhibited the finest grain size. The pure Mg material exhibited a grain size of 243 μm (Table 1). Thus, Zn is a potent grain refiner for Mg where 4 wt.% refined the grain size the greatest amount for the range of Zn compositions studied.

3.2. Properties

3.2.1. Tension

The RT tensile properties, including YS, UTS, and ε_f for selected microstructures are listed in Table 2. Fig. 5 compares the RT tensile strength values. The strengths values were similar for Zn concentrations between 2.9 and 4.1, while the Mg–4.4Zn alloy exhibited significantly lower strength values. However, the strength of the Mg–4.4Zn alloy was greater than that for

Table 2
RT tensile properties

Alloy	0.2% YS (MPa)	UTS (MPa)	ε_f (%)
Mg	61	102	1.5
Mg–2.9Zn	84	219	4.7
Mg–3.3Zn	90	210	4.6
Mg–4.0Zn	95	216	4.1
Mg–4.1Zn–0.2Y	98	223	5.0
Mg–4.4Zn	68	155	8.4

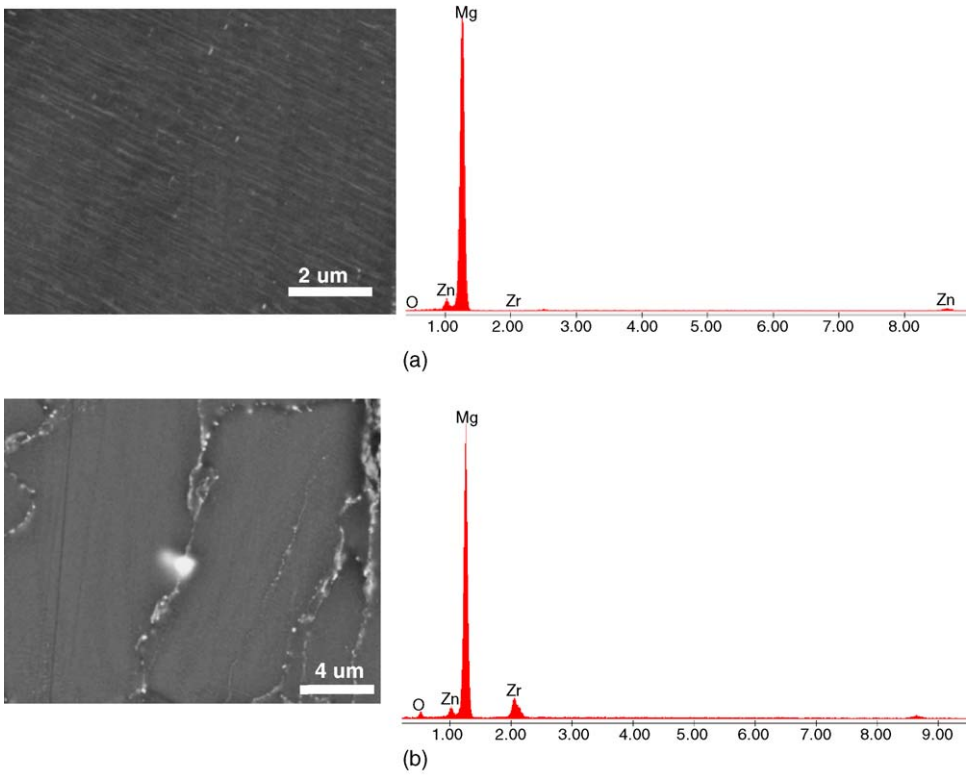

Fig. 3. SEM and EDS analysis of Mg–3.6Zn illustrating the (a) matrix composition enriched in Mg and Zn and a (b) grain boundary particle (light contrast) enriched in Zr, Mg, and Zn.

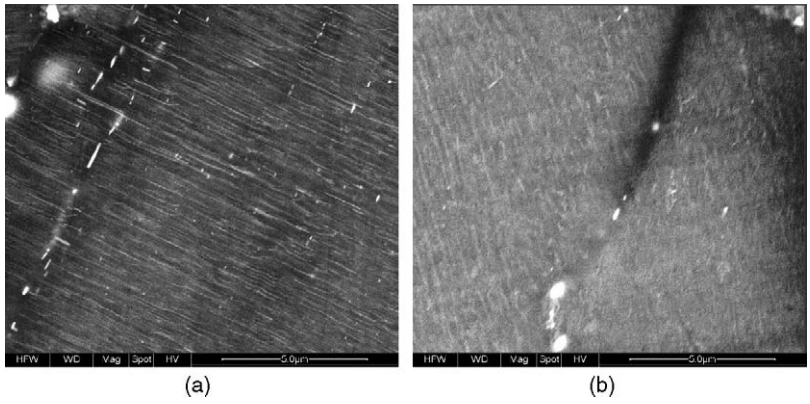

Fig. 4. Fine nanometer size laths/platelets were exhibited for (a) Mg–4.1Zn–0.2Y and (b) Mg–2.9Zn.

Mg. The ε_f values tended to increase with increased Zn over the entire range of Zn added, where Mg–4.4Zn exhibited a ε_f value of 8.4%. The Mg samples exhibited the lowest average ε_f value, 1.5%. Thus, Zn increased each of the YS, UTS, and ε_f values. The 150 °C tensile results (see Table 3) are exhibited in Fig. 6. Each of the materials exhibited lower strengths than at RT, and the 150 °C ε_f values tended to be larger than those measured at RT. In this case, Zn compositions between 4.0 and 4.4 exhibited superior strength values compared with the other alloys and pure Mg. Tensile fracture surfaces of the specimens depicted a combination of ductile dimpling and cleavage (see Fig. 7). Combining the RT and 150 °C tensile observations, the Mg–4.1Zn–0.2Y alloy exhibited the greatest strength of all the alloys. Fig. 8 illustrates the effect of temperature on the UTS and YS. The pure Mg material exhibited the lowest strength and ε_f values. The Mg–4.1Zn–0.2Y alloy exhibited over 1.5 times the strength and ε_f of the pure Mg material. Thus, similar to that observed for Mg–Y alloys [13,17], Zn is a potent strengthener

Table 3
150 °C tensile properties

Alloy	0.2% YS (MPa)	UTS (MPa)	ε_f (%)
Mg	50	62	1.8
Mg–2.9Zn	43	62	16.9
Mg–3.3Zn	82	93	1.6
Mg–4.0Zn	84	111	4.4
Mg–4.1Zn–0.2Y	78	116	5.4
Mg–4.4Zn	79	114	5.2

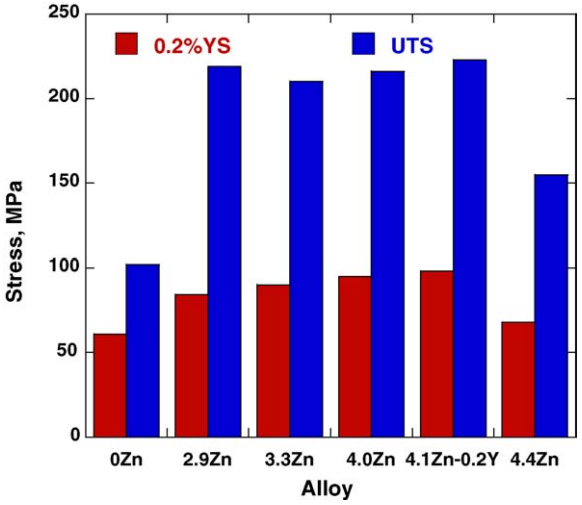

Fig. 5. RT tensile results for the studied materials.

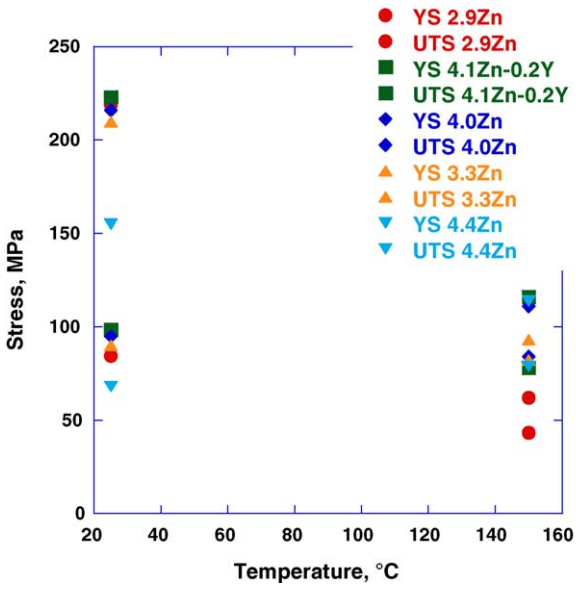

Fig. 8. UTS and YS vs. temperature plot for the studied alloys.

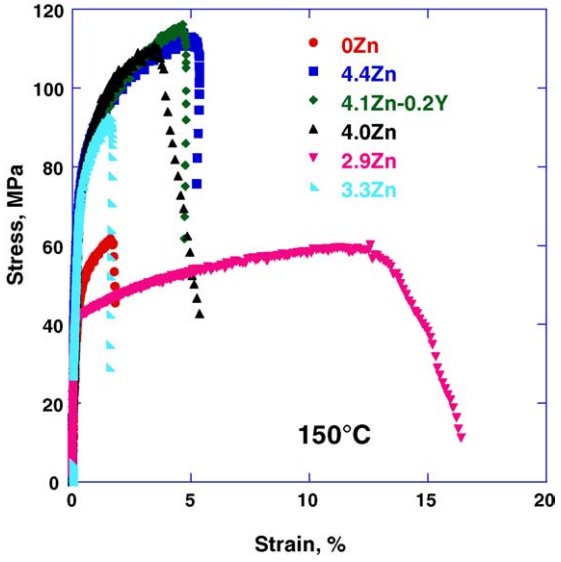

Fig. 6. Representative tensile stress vs. strain curves for the studied alloys at 150 °C.

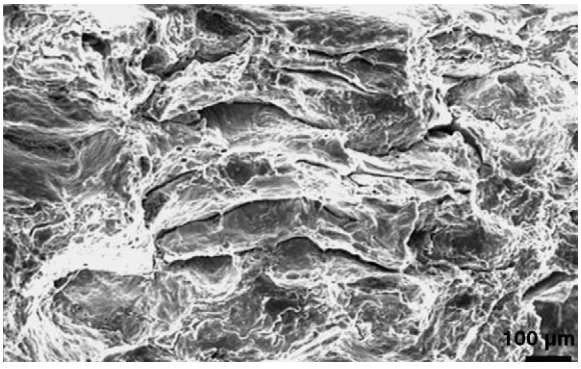

Fig. 7. SEM images of the 150 °C tensile fracture surface of a Mg–4.4Zn sample which failed at 5.2% strain.

for Mg and for the range of compositions examined, 4.1 wt.% Zn provided the greatest strengthening.

3.2.2. Creep

The creep strain-life behavior resembled that for most pure metals and alloys [21], where the primary, secondary, and tertiary stages were each represented. Fig. 9 illustrates a typical creep strain versus time curve of an Mg–3.3Zn alloy. Fig. 10 illustrates creep strain versus time plots for the Mg–2.9Zn and Mg–4.1Zn–0.2Y specimens tested at 150 °C/30 MPa. The Mg–4.1Zn–0.2Y alloy proved to be the most creep-resistant among all the alloys tested when both total creep extension and secondary creep rate were considered. Comparing the minimum creep rates (Table 4), the Mg–2.9Zn exhibited creep resistance superior to Mg–3.3Zn. It is noted that pure Mg was not creep tested. SEM analysis of the Mg–4.1Zn–0.2Y alloy microstructure did not reveal any microstructural change or cracking (Fig. 11). Creep fracture surfaces of the Mg–2.9Zn specimen

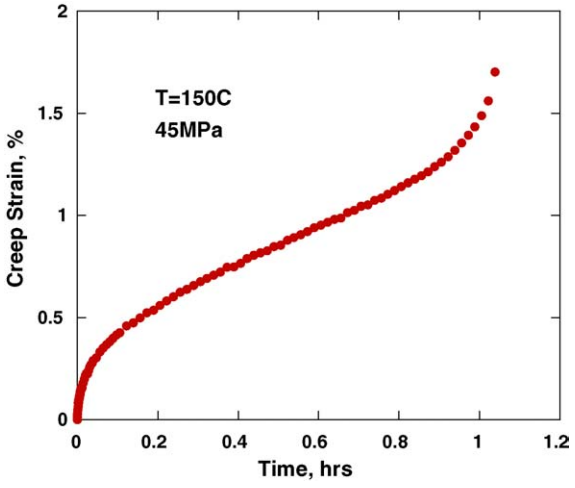

Fig. 9. Creep strain vs. time plot for a Mg–3.3Zn sample at 150 °C/45 MPa.

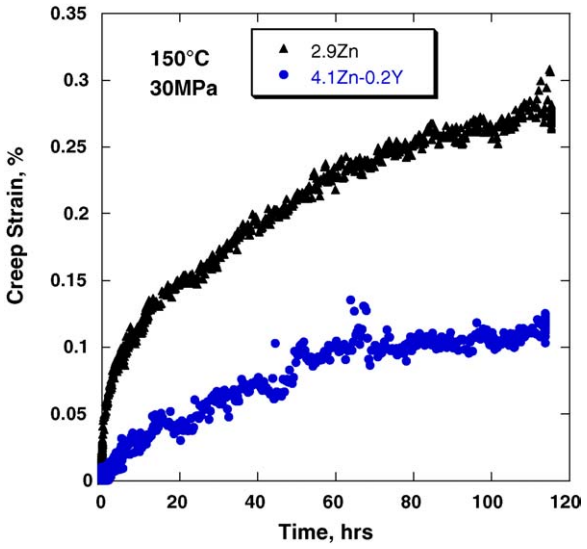

Fig. 10. Creep strain vs. time plots for Mg–Zn alloys at 30 MPa and 150 °C.

Table 4
Measured creep steady-state strain rates

Alloy	σ/T (MPa/°C)	$\dot{\varepsilon}_{min}$ (s^{-1})
Mg–2.9Zn	30/150	1.97E−09
Mg–3.3Zn	45/150	2.52E−06
Mg–4.1Zn–0.2Y	30/150	7.29E−10
Mg–4.1Zn–0.2Y	40/150	2.70E−09
Mg–4.1Zn–0.2Y	50/150	6.10E−09

depicted a greater volume of cleavage-type brittle fracture than ductile dimpling (see Fig. 12).

The creep parameter n was determined using the following creep-law equation:

$$\dot{\varepsilon}_{min} = B\sigma^n \quad (1)$$

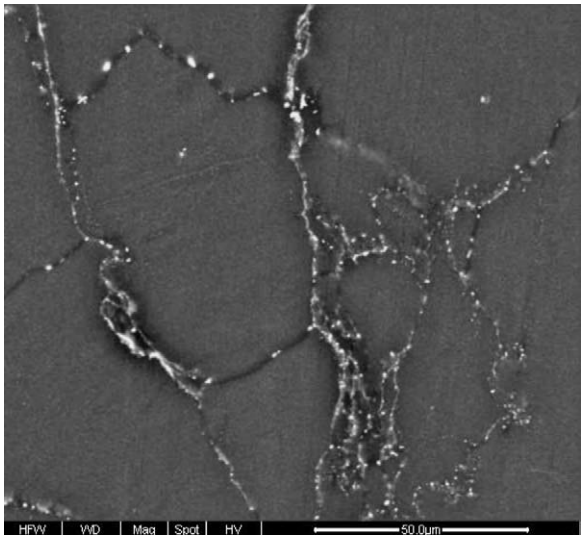

Fig. 11. SEM image of a Mg–4.1Zn–0.2 alloy after creep deformation between 30 and 50 MPa at 150 °C to $\varepsilon = 0.25\%$ for 236 h.

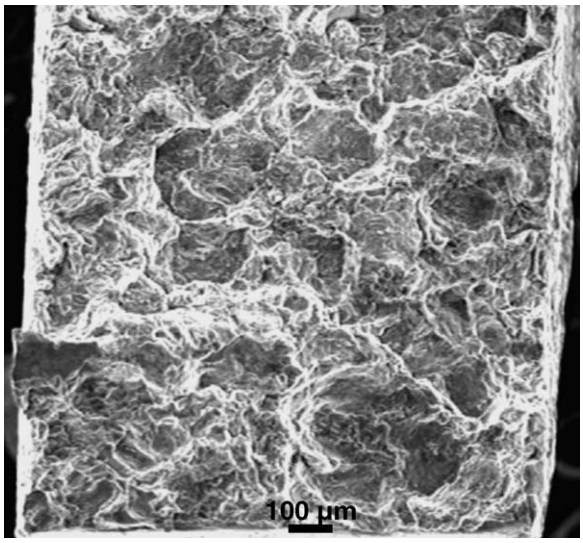

Fig. 12. SEM images of the creep fracture surface of a Mg–2.9Zn sample which failed after 0.34% strain after 117 h at 150 °C (30 MPa).

where B is a material-related constant; σ is the applied stress, and n is the creep stress exponent. In this study, the n value was obtained in order to reveal the possible creep mechanisms involved. Table 4 lists the testing conditions and $\dot{\varepsilon}_{min}$ for each of the specimens tested. Fig. 13 illustrates the stress dependence on $\dot{\varepsilon}_{min}$. For the Mg–4.1Zn–0.2Y alloy, n was 4.2, which suggests a dislocation climb mechanism is active. This has been suggested previously for Mg-based alloys under similar test conditions [2,22]. In both ingot and die cast AZ91, creep mechanisms based on dislocation motion (on basal and non-basal planes) were proposed [23,24]. In addition, 377 °C creep investigation of Mg–Y–Zn alloys revealed that higher dislocation densities, up to a factor of two, were present in the alloys containing Zn compared to those without Zn [13]. The high dislocation density was suggested to be one of the reasons for the improved creep resistance of the Zn-containing alloys. In addition, the strengthening effects of Zn have been considered due to the decrease in stacking fault energy and consequent reduction of mobility of the dislocations [17]. Thus, alloying with Zn leads to increasing

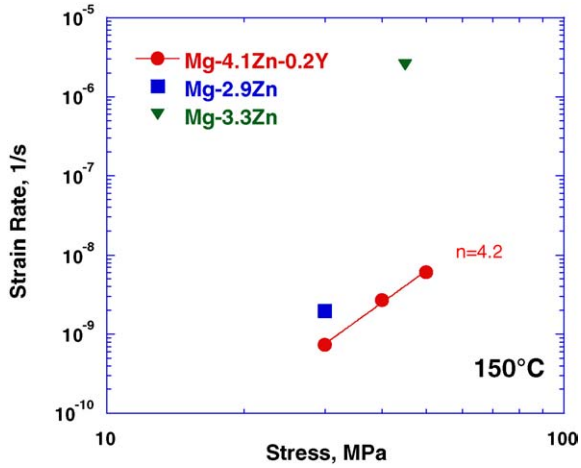

Fig. 13. Log minimum strain rate vs. log stress for the Mg–Zn alloys at 150 °C.

both the strength and creep resistance of Mg, and 4.1 wt.% Zn resulted in the greatest strengthening of all the alloys examined. At this point, the effect of Y on the strengthening could not be delineated and will be the focus of a forthcoming work.

4. Conclusions

1. The Mg–Zn alloy microstructures contained equiaxed grains where the finest grain sizes were observed for the Mg–4Zn alloy. Nanometer size laths were observed in two of the alloys (Mg–2.9Zn and Mg–4.1Zn–0.2Y).
2. The tensile strength of the Mg–4.1Zn–0.2Y alloy was the greatest at both RT and 150 °C. The RT ε_f values tended to increase with increased Zn over the entire range of Zn added, where Mg–4.4Zn exhibited a ε_f value of 8.4%. Zn alloying resulted in an over 1.5 times increase in strength and ε_f compared to that for the baseline Mg material.
3. The tensile–creep properties of Mg–4.1Zn–0.2Y were significantly better than those of the other Mg–Zn alloy compositions evaluated.
4. The stress dependency of the secondary creep rate at 150 °C suggests that the alloys experience a dislocation-controlled creep mechanism for stresses between 30 and 50 MPa.
5. Overall, Zn was observed to be a potent strengthener for Mg, where 4.1 wt.% resulted in the greatest improvement in tensile and creep properties.

Acknowledgments

This work was partially supported by the National Science Foundation through grant DMR-0320992. The authors are grateful to Daniel Burnett III, Matthew Dispenza and John Rich (Alfred University), and Christopher Cowen (Michigan State University) for their technical assistance.

References

[1] B.R. Powell, A.A. Luo, V. Rezhets, J.J. Bamarito, B.L. Tiwari, Society of Automotive Engineers (2001), paper #2001-01-0422.
[2] A.A. Luo, M.P. Balogh, B.R. Powell, Society of Automotive Engineers (2001), paper #2001-01-0423.
[3] B.R. Powell, V. Rezheiss, M. Balogh, R. Waldo, Magnesium Technol. (2001) 175–182.
[4] L.L. Rokhlin, Magnesium Alloys Containing Rare Earth Metals Structure and Properties, Taylor and Francis, New York, NY, 2003, p. 211.
[5] I.P. Moreno, K.Y. Sohn, J.W. Jones, J.E. Allison, Society of Automotive Engineers (2001), paper #2001-01-0425.
[6] I.P. Moreno, T.K. Nandy, J.W. Jones, J.E. Allison, T.M. Pollock, Scripta Mater. 48 (2003) 1029–1034.
[7] S.M. Zhu, X. Gao, J.F. Nie, Mater. Sci. Eng., A 384 (2004) 270–274.
[8] V. Sklenicka, M. Pahutova, K. Kucharova, M. Svoboda, T.G. Langdon, Metall. Trans. 33A (2002) 883–889.
[9] A.A Luo, T. Shinoda, Society of Automotive Engineers (1998), paper #980086.
[10] A.A. Luo, B.R. Powell, Magnesium Technol. (2001) 137–144.
[11] E. Baril, P. Labelle, M.O. Pekguleryuz, J. Met. (2003) 34–39.
[12] K. Ozturk, Y. Zhong, A.A. Luo, Zi-Kui Liu, J. Met. (2003) 40–44.
[13] K. Maruyama, M. Suzuki, H. Sato, Metall. Mater. Trans. 33A (2002) 875.
[14] M. Suzuki, T. Kimura, K. Maruyama, H. Oikawa, Mater. Sci. Eng. A252 (1998) 248–255.
[15] M. Suzuki, T. Kimura, J. Koike, K. Maruyama, Mater. Sci. Eng., A 387–389 (2004) 706–709.
[16] M. Suzuki, T. Kimura, J. Koike, K. Maruyama, Scripta Mater. 48 (2003) 997–1002.
[17] M. Suzuki, T. Kimura, J. Koike, K. Maruyama, Mater. Sci. Forum 426–432 (2003) 593–598.
[18] M. Suzuki, R. Inoue, M. Sugihara, H. Sato, J. Koike, K. Maruyama, H. Oikawa, Mater. Sci. Forum 350–351 (2000) 151.
[19] T. Sato, Mater. B Jpn. Inst. Met. l38 (1999) 294.
[20] Standard Test Methods for Determining Grain Size Designation E112-88, American Society for Testing and Materials (ASTM), West Conshohocken, PA, 1988, pp. 228–253.
[21] R.W. Evans, B. Wilshire, in: D. McLean (Ed.), Creep of Metals and Alloys, The Institute of Metals, 1985, pp. 295–307.
[22] M.S. Dargusch, G.L. Dunlop, in: B.L. Mordike, K.U. Kainer (Eds.), Magnesium Alloys and Their Applications, Werkstoff-Informationsgesellschaft, Frankfurt, Germany, 1998, pp. 277–282.
[23] M. Regev, E. Aghion, A. Rosen, M. Bamberger, Mater. Sci. Eng. A252 (1998) 6–16.
[24] M. Regev, E. Aghion, A. Rosen, Mater. Sci. Eng. A234–236 (1997) 123–126.